Degradation of polyamide nanofiltration membranes by bromine: changes of physiochemical properties and filtration performance

Huihui Zhao [a], Linyan Yang *[,a,b,c], Xueming Chen [d], Mei Sheng [a], Guomin Cao [a,b,c], Lankun Cai [a,b], Shujuan Meng [e], Chuyang Y. Tang [f]

[a] School of Resources and Environmental Engineering, East China University of Science and Technology, Shanghai 200237, P.R.China

[b] National Engineering Laboratory for Industrial Wastewater Treatment, East China University of Science and Technology, Shanghai 200237, PR China

[c] Shanghai Institute of Pollution Control and Ecological Security, Shanghai 200092, P.R. China

[d] Fujian Provincial Engineering Research Center of Rural Waste Recycling Technology, College of Environment and Resources, Fuzhou University, Fuzhou, Fujian, 350116, P.R. China

[e] School of Space and Environment, Beihang University, Beijing 100191, P. R. China

[f] Department of Civil Engineering, University of Hong Kong, Pokfulam, Hong Kong

Corresponding Author

*Phone: +86-13270696038; e-mail: lyyang@ecust.edu.cn

20

Graphical abstract

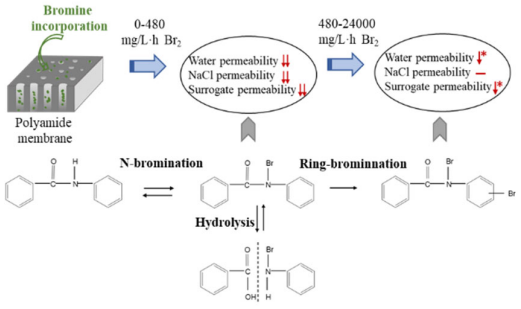

21

Abstract

The potential coexistence and interaction of bromine and polyamide membranes during membrane-based water treatment prompts us to investigate the effect of bromine on membrane performance. For fully aromatic polyamide membrane NF90 exposed under a mild bromination condition (10 mg/L), bromine incorporation resulted in more negatively charged (–13 mV vs. –25 mV) and hydrophobic (55.2 º vs. 58.9 º) surfaces and narrower pore channels (0.31 nm vs. 0.29 nm). The permeabilities of water and neutral solutes were reduced by 64% and 69%–87%, respectively, which was attributed to the decreased effective pore radius and hydrophilicity. NaCl permeability was reduced by 90% as a synergistic result of enhanced size exclusion and charge repulsion. The further exposure (100 and 500 mg/L bromine) resulted in a more hydrophobic surface (61.7° and 65.5°) and the minor further reduction for water and solute permeabilities (1%–9%). Compared with chlorine, the different incorporation efficiency and properties (e.g., atomic size, hydrophilicity) of bromine resulted in opposite trends and/or different degrees for the variation of physicochemical properties and filtration performance of membranes. The bromine incorporation, the shift and disappearance of three characteristic bands, and the increased O/N ratio and calcium content indicated the degradation pathways of N-bromination and bromination-promoted hydrolysis under mild bromination conditions (480 mg/L·h). The further ring-bromination occurred after severe bromine exposure (4800–24000 mg/L·h). The semi-aromatic polyamide membrane NF270 underwent a similar but less significant

43 deteriorated filtration performance compared with NF90, which requires a different
44 explanation.
45

Introduction

The polyamide-based thin film composite (TFC) membranes have been widely applied in (waste) water treatment and seawater desalination due to their excellent permeability and selectivity.[1-3] The polyamide top layer with a thickness of a few hundred nanometers is responsible for membrane performance.[4] However, the weak resistance of polyamide materials to oxidizing agents (e.g. chlorine, bromine and hydrogen peroxide [5, 6]) reduces the membrane lifespan and complicates the membrane-based treatment process. For example, a pre-disinfection step to prevent biofouling often requires a disinfectant removal step prior to the membrane system to protect the downstream polyamide membranes (a common practice in seawater desalination). Nevertheless, the inevitable disinfectant residuals are still able to degrade membrane materials.

Chlorine is commonly used as a disinfectant for biofouling control and as a membrane cleaning agent. Compared with chlorine-based disinfectants, bromine-based counterparts are widely used for industrial wastewater (mainly in water fountains and cooling towers), spa and swimming pool water disinfection considering their lower toxicity, higher chemical stability with less odor, greater reactivity, and more efficient bactericide.[7-10] In spite of direct bromine addition, hypobromous acid (a predominant oxidizing agent) can be formed after the addition of chlorine to bromide ion-containing (waste) water, such as seawater disinfection.

Although the effect of chlorine on polyamide membrane degradation has been extensively investigated[11, 12], the underlying mechanism of the reaction between bromine and polyamide membranes is yet fully understood.[13] Despite the apparent similarity of extremely strong electron affinities for chlorine and bromine [14], the latter with a weaker electronegativity, a larger atomic radius, and a higher halogenation reactivity may result in contrasting halogenation reactions.[13, 15] Bromine-based substitution reaction for model compounds and natural water has proven to be faster and more effective than chlorine-based counterpart.[16] Similarly, bromine incorporation into membranes is more favored than chlorine even with an excess amount of free chlorine, which results in greater changes for water flux and solute rejection.[17, 18] Assuming the similar degradation pathway of large organic molecules (e.g., amino acids, peptides and proteins) by active halogen, i.e., HOBr and HOCl,[19, 20] the degradation pathways of polyamide membranes have been considered as N-bromination and the accompanying ring-bromination via Orton rearrangement based on the commonly accepted membrane chlorination mechanism. However, Glater et al.[21] found that bromine incorporation to polyamide membranes occurs directly on aromatic rings by electrophilic substitution. Therefore, the fundamental mechanism for membrane bromination is worthy of deeper investigation.

The potential interaction between polyamide membranes and bromine and the

contradictory findings and explanation of bromination pathways prompted a systematic investigation on polyamide membrane degradation by bromine. Briefly, physicochemical properties and filtration performance of virgin and brominated polyamide-based nanofiltration membranes (i.e., NF90 and NF270) were characterized. By comparing the bromination-based results obtained in this study with the chlorination-based ones extracted from a reference,[12] we proposed the degradation mechanism of polyamide membranes by bromine. The fundamental understanding of membrane degradation by different oxidizing agents is essential for simplifying membrane-based (waste)water and seawater treatment process, the proper selection of disinfectants or cleaning agents, and the fabrication of oxidant-resistant membrane materials.

Materials and methods

Chemicals and materials

The bromine reagent-1,3-dibromo-5,5-dimethylhydantoin (DBDMH, an alternative reagent for bromine disinfection [22, 23]) with a purity of 98% obtained from Aladdin Biotechnology was used in this study. Converting bromide using chlorine is technically feasible to produce active bromine, but the introduction of chlorine may cause some uncertainty (i.e., the potential formation of other active components [24-26]). Sodium chloride (>99.5%) was used to evaluate the bromination effect on the salt rejection of membranes. Three neutral surrogates including glycerol, erythritol, and glucose (with

109 a purity over 98%) were purchased from Adamas-beta Reagent except erythritol from
110 Dubai Biotechnology. They were used as the probing molecules to evaluate the
111 bromination effect on effective membrane pore radii. Three hydrophobic hormones
112 (bisphenol-A, dienestrol and estriol) with a purity of over 98% were purchased from
113 Aladdin Technology. Calcium chloride (>96%) was used to determine the amount of
114 membrane carboxyl functional groups. [12] Hydrochloric acid (37%) and sodium
115 hydroxide (>96%) were used for pH adjustment. All the chemicals used in this study
116 were of analytical grades. Deionized (DI) water (conductivity < 4.0 μs/cm) was used in
117 all stock solution preparations and experiments.
118
119 Two commercial TFC nanofiltration membranes, namely, NF90 and NF270, obtained
120 from Dow Filmtec were investigated in this study. The fully aromatic polyamide
121 membrane NF90 was prepared by 1,3-benzenediamine and trimesoyl chloride and the
122 semi-aromatic polyamide membrane NF270 was fabricated by piperazine (PIP) and
123 trimesoyl chloride.[27-29] The membrane structures and properties are shown in
124 Supporting Information S1 and Table 1, respectively. The membranes were stored at 4
125 ºC in the dark.
126
127 Table 1. Membrane properties

Membrane	Surface Layer material	Water permeability[a] L/(m^2 h bar)	Salt rejection[b] %	Zeta potential[c] mV	Contact angle[d] °	Surface Roughness[d] nm	Pore radius[e] nm

NF90	Fully aromatic polyamide	9.0	87.4	-13	55.2±2.5	64.9±8.1	0.31
NF270	Semi-aromatic polyamide	17.5	56.3	-53	18.3±2.6	5.1±0.5	0.40

Notes:

[a] Water permeability was recorded after 24 hours' membrane compaction under the following conditions (100 psi, 25 ºC, 1 L/min, pH 7.5, DI water).

[b] Salt rejection was determined after NaCl was added to the feed tank for 24 h under the following conditions (100 psi, 25 ºC, 1 L/min, pH 7.5, 10 mM NaCl).

[c] Zeta potential was measured at pH=7.5 with 10 mM NaCl as the background electrolyte.

[d] The contact angle and surface roughness were measured for the vacuum dried membrane coupons after 24 hours' exposure in DI water.

[e] The membrane effective pore radius was calculated according to a solute transport model based on the filtration tests of three surrogates in this study.[30]

Membrane bromination procedures

The membrane coupons were soaked in DI water for 24 h before being exposed in bromine solution with a series of concentrations, i.e., 0 (as control), 10, 100, and 500 mg/L. The bromine concentration was determined photometrically by the dipropyl-p-phenylenediamine method (Spectroquant® chlorine test, EPA 330.5, Merck) and reported equivalently to mg/L as Cl_2 - a unit commonly used to characterize the concentration of disinfectants). The solution pH was adjusted to 7.5 by 0.1 M HCl and NaOH. The membrane exposure experiments were conducted in 250 ml amber glass bottles with PTFE-lined caps to minimize bromine self-degradation. The bromine depletion after each experiment was within 5%–9%, which was similar to the reported values in literature.[31, 32] The sample bottles were oscillated on a shaker (HZP-250, Jinghong Laboratory Equipment, China) working at a rotating speed of 120 r/min at an

ambient temperature of ~25 °C for 48 h. In the current study, the bromine exposure was evaluated as the product of bromine concentration and exposure time (CT), which is commonly adopted for evaluating membrane tolerance to chlorine using accelerated testing conditions.[12, 32] In addition, accelerated membrane degradation directly in membrane system is not desirable since bromine with extremely high concentration may damage the membrane setup. The brominated membrane samples were rinsed with DI waters for 5 times to remove bromine residuals and vacuum-dried for XPS, FTIR, SEM, AFM, and contact angle measurement. Zeta potential was measured for wet samples.

Membrane characterization

X-ray photoelectron spectroscopy (XPS)

The chemical composition of the membrane surface from the top 0–5 nm was measured by XPS (ThermoFischer Escalab 250Xi, USA). To evaluate the bromination effect on bromine incorporation into the membrane matrix and membrane surface carboxylic groups, the virgin and brominated membrane coupons were immersed in 0.1 mM $CaCl_2$ at pH 7.5 for 2 times (each for 10 min) and rinsed in 0.001 mM $CaCl_2$ at pH 7.5 for 5 times (each for 5 min) to remove Ca^{2+} not bound to the membrane surface.[12, 32] The membranes were dried in vacuum before XPS analysis. Five elements including C 1s, N 1s, O 1s, Br 3d and Ca 2p were monitored. The signal was accumulated in 10 cycles under a vacuum environment (8×10^{-10} Pa) with 12.5 kV working voltage and 16 mA

filament current with aluminum Kα radiation as an X-ray source at 1486.6 eV. The passing-energy was tested at 40 eV with a step size of 0.1 eV. The combined energy standard C 1s = 284 eV was used for charge correction.

Attenuated total reflection-Fourier transform infrared (ATR-FTIR)

The binding chemistry of virgin and brominated membranes was characterized by an FTIR spectrometer (IS5, Nicolet, America) equipped with a 45° multi-reflection HART flat plate crystal (PIKE Technologies, America) as ATR element and an Omnic 8.2 software (Thermo Electron Corporation). The spectrum in an absorption mode was averaged from 50 scans over the range of 600 cm^{-1}–4000 cm^{-1} at 2 cm^{-1} resolution. The instrument was continuously purified with dry air to prevent the exposure of the sample to the atmospheric moisture.

Field emission scanning electron microscopy (FE-SEM)

The membrane surface topography was monitored by FE-SEM (Gemini SEM 500, AEISS, German). The virgin and brominated dry membranes were attached to a metal sample table by copper adhesive to form a conductive path. The membrane surface was coated with a layer of gold by a sputter coater for 10 s before measurements.

Atomic force microscope (AFM)

AFM working in a contact mode in air was used to determine the surface roughness of

193 virgin and brominated membranes (Veeco DI, America). The root-mean-square surface
194 roughness (R_{rms}) was obtained from AFM feature height distribution data.[33]
195
196 **Contact angle**
197 Contact angles for virgin and brominated membranes were measured by a goniometer
198 (JY-82B, China). The vacuum dried membrane samples were attached to a glass slide
199 to obtain a flat surface before analysis. A syringe filled with DI water was used to drip
200 a droplet of 10 μL DI water onto the membrane surface. The contact angle of each
201 sample was obtained from 20 measurements at different locations to eliminate the
202 measurement uncertainty.
203
204 **Zeta potential**
205 The membrane surface charge was quantified by a SurPass electrokinetic analyzer
206 (Anton Paar GmbH, Austria). The 10 mM NaCl was used as a background electrolyte
207 and the pH varying from 3.0 to 10.0 was adjusted by 0.1 M HCl and NaOH. The zeta
208 potential was calculated by the Helmholtz–Smoluchowski equation.[34] The reported
209 surface charge was the average of two independent measurements.
210
211 **Membrane filtration experiments**
212 **Membrane setup**
213 The membrane filtration system contained four parallel rectangular cross-flow

membrane cells (CF042, Sterlitech, USA) with a channel size of 4.6 cm × 9.2 cm (an effective membrane surface area of 42 cm^2). A medium foulant spacer with a thickness of 1.2 mm (CF042, 47 mil, Diamond, Sterlitech, USA) was placed in each cell. The temperature of feed solution was controlled at 25 ºC by a chiller (CW-5200, Teyu electrical, China). The permeate and concentrate were recirculated back to the feed tank during the entire experiment.

Filtration experiments

The virgin and brominated membranes were rinsed by DI water for 24 h before filtration experiments. The membranes were loaded into the cells and compacted for at least 12 h before sample collection to eliminate the compaction effect. Filtration tests were performed at a pressure of 100 psi, a system temperature of 25 ºC, and a cross-flow velocity of 1 L/min (corresponding to a superficial velocity of 22.6 cm/s). The solution pH was adjusted to 7.5 by 1 M HCl and NaOH.

Three kinds of feed solutions, i.e., DI water, a solution with 5 mM or 50 mM NaCl, and a solution with 200 mg/L of each surrogate, were used to determine pure water, salt, and surrogate permeability for virgin and brominated membranes, respectively (the calculation formulas can be found in Supporting Information S2). The same membrane coupon was used for different feed tests to minimize the minor material difference of different regions. Upon the changes of feed solutions, the filtration setup was run for 6

h to stabilize the system. The water permeability was measured by weighting the mass of permeate at a time interval of 10 min. The salt permeability was determined by measuring the conductivity of feed and permeate samples by a conductivity meter (Ultrameter II 4p, Myron L, USA). The neutral surrogate permeability was evaluated by testing the surrogate concentration of feed and permeate by a total organic carbon (TOC) analyzer (TOC-V CPN, Shimadzu, Japan) equipped with an auto-sampler (ASI-V, Shimadzu, Japan). The permeability of each surrogate was tested separately. The filtration tests for hormone solution were performed to evaluate the hydrophilic properties of brominated membranes. The hormones were measured by liquid chromatography tandem mass spectrometry (LC-MS/MS, LCMS-8050, Shimadzu, Japan) using electrospray ionization (ESI) in a negative mode coupled with a Shimadzu-pack GISS C18 column (2.1 × 100 mm, 1.9 μm). The pretreatment and analytical methods can be found elsewhere. [35]

Results and discussion

Effect of bromination on membrane physicochemical properties

Changes in membrane surface morphology

The virgin NF90 membrane had a rough surface (reflected by an RMS roughness of 64.9 nm, Table 1) with a ridge-and-valley structure (refer to the SEM and AFM profiles in Supporting Information S3 and S4). The virgin NF270 membrane presented a smoother surface with an RMS roughness of only 5.1 nm. Notably, roughness features on NF90 surfaces became more compact after bromination (500 mg/L for 48 h, 82.4

nm vs. 64.9 nm, $p \leq 0.05$, ANOVA, Supporting Information S5), which was in accordance with a polyamide membrane (ESPA2) degraded by chlorine.[36] For brominated NF270, remarkable cracks on material surfaces were observed although the surface roughness did not show a significant difference, which demonstrates that surface layer was partially collapsed/destroyed (Supporting Information S3).

Changes in membrane surface chemistry

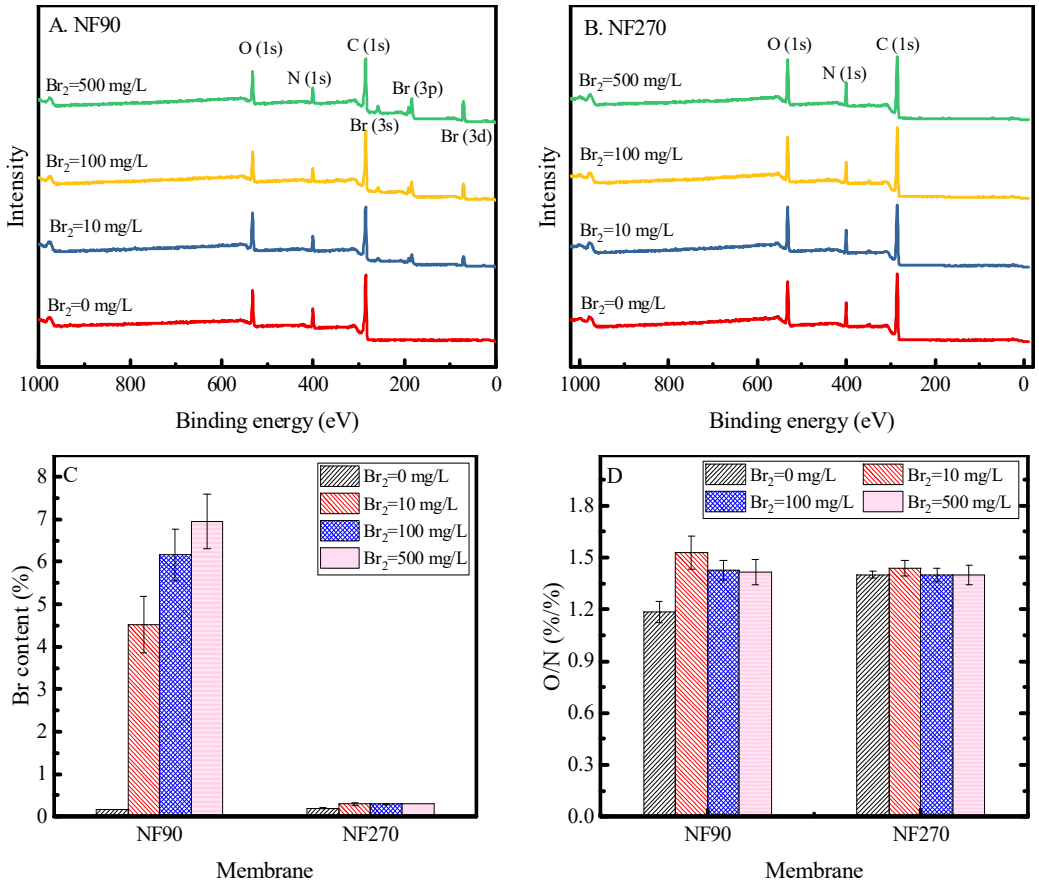

Figure 1. Effect of bromination on XPS spectra (A, B) and bromine content on the membrane surface (C) and ratio of oxygen to nitrogen (D) for NF90 and NF270. Membranes were exposed to bromine at 0, 10, 100, and 500 mg/L for 48 h, pH 7.5, 25 ºC. The error bars represented the range based on two independent experiments.

The bromine peaks in XPS spectra were revealed at binding energies of ~255 eV (3s), ~182 eV (3p), and ~75 eV (3d) for brominated NF90 membranes, while such peaks were not obviously observed for the virgin one (Figure 1A). The bromine content increased dramatically from 0.2% (for control) to 4.5% for NF90 exposed under a mild bromination condition (10 mg/L, Figure 1C and Supporting Information S6). The further increase in bromine concentration up to 500 mg/L only resulted in a bromine content of 7.0%. In addition, the number of carboxylic groups for NF90 increased remarkably after 10 mg/L bromine exposure and remained constant after further exposure (reflected by Ca content determined by XPS, Supporting Information S6). The reactive sites for bromine incorporation might be saturated and/or reaction transformation might occur under severe bromination conditions (see further discussion in next section). The bromine content for virgin and brominated NF270 ($\leqslant$0.3%) did not show a significant difference (Figure 1B, C and Supporting Information S6), which was attributed to the higher chemical inertia of the aliphatic tertiary amine nitrogen in NF270 than amide nitrogen in NF90 to bromine attack. [32, 37, 38] Simon et al.[39] similarly observed an extremely weak chlorine uptake by NF270.

The atomic O/N ratio, which is commonly used to assess the degree of cross-linking for polyamide layers, [32] was used to evaluate the degree of membrane bromination (Figure 1D). According to literature reports, chlorinated polyamide membranes may encounter amide C-N bond breakage and additional carboxyl group formation, which

is reflected by the increased O/N ratio (the introduction of oxygen elements, which results in a less cross-linked polyamide structure).[12, 32] In the current study, the O/N ratio increased from 1.2 for virgin NF90 to 1.5 for membranes treated by 10 mg/L bromine, then the ratio kept nearly constant after further exposure (100 and 500 mg/L) despite of the further bromine incorporation (Figure 1C). Based on N-chlorination mechanism[32], it is speculated that N-bromination may reach saturation under a mild bromination condition and the further exposure may result in other bromination mechanism. The O/N ratio for virgin and brominated NF270 was nearly constant at ~1.4 due to the stability of tertiary amide bonds of the PIP PA layer at neutral pHs, [40] which is consistent with bromine content results.

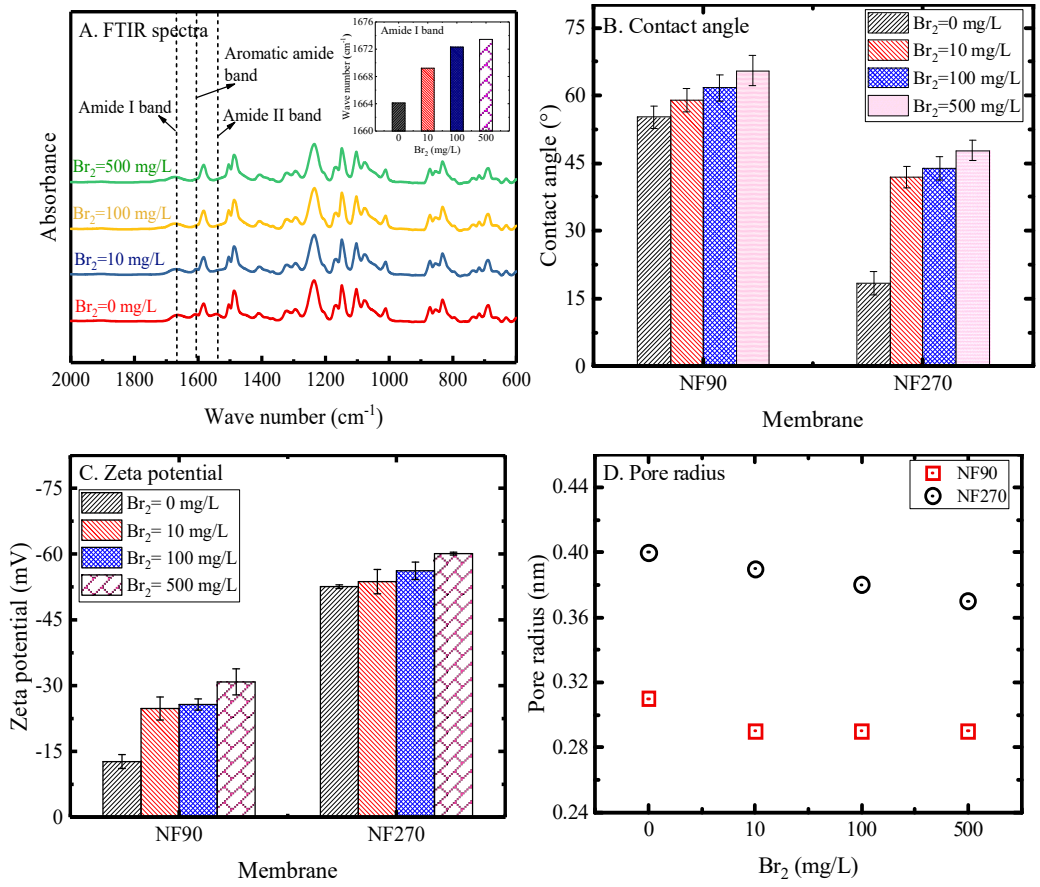

Figure 2. Effect of bromination on ATR-FTIR absorption spectra (the shifted wave number of amide I band was shown on the top-right) (A), contact angles (B), zeta potential (C) and effective pore radius (D) for NF90 and NF270. Membranes were exposed to bromine at 0, 10, 100, and 500 mg/L for 48 h, pH 7.5, 25 ºC. The contact angles were the average of twenty independent measurements. The error bars for zeta potential represented the range based on two independent experiments (10 mM NaCl, pH 7.5). The effective pore radius was calculated by a transport model developed by Nghiem.[30]

FTIR results show that the fully aromatic polyamide chemistry for NF90 was characterized by absorption bands of 1664 cm^{-1} (amide I band), 1541 cm^{-1} (amide II band) and 1609 cm^{-1} (aromatic amide band)[41] (Figure 2A). The peak of amide I band (assigned to C=O stretching, the C–N stretching and the C–C–N deformation vibration [42]) was shifted to a higher wave number, from 1664 cm^{-1} to 1669 cm^{-1} after exposure for 48 h under 10 mg/L bromine. Another 5 cm^{-1} shift was observed when the bromine concentration further increased to 500 mg/L (see the up-right of Figure 2A). The breakage of hydrogen bonds between C=O and N–H groups and the additional carboxyl groups formed by hydrolysis may contribute to this shift given that the C=O stretching of benzoic acid is at 1680 cm^{-1}. [32] In other words, the formation of hydrogen bonds between C=O and N–H groups in NF90 led to a shift of C=O adsorption band to a lower wave number. [43, 44] The hydrogen bond breakage and additional carboxyl group formation after bromination resulted in a back shift. The disappearance of amide II band (assigned to N–H in plane bending and N–C stretching vibration of a –CO–NH– group [43, 44]) and aromatic amide band (assigned to the N–H deformation vibration[43] or C=C ring stretching vibration [45]) may suggest that the hydrogen on amide groups and

aromatic rings was replaced by bromine via electrophilic substitution (i.e., N-bromination and ring-bromination). The unchanged spectra for brominated NF270 membranes (Supporting Information S7) further demonstrated the resistance of tertiary amine and aliphatic rings in piperazinyl polyamide to bromine, [46] which is consistent with the negligible bromine attack and constant O/N ratio (Figure 1C, D).

Changes in membrane hydrophilicity and charge

The contact angle for NF90 increased significantly after the membranes were exposed in bromine solutions (Figure 2B), which implies a reduced hydrophilicity (weaker wettability) for brominated membranes. The bromine incorporation contributes to a more hydrophobic membrane surface.[12, 47] Nevertheless, the increased number of carboxylic groups (reflected by the increased Ca content determined by XPS, Supporting Information S6) may somehow result in a stronger wettability. The enhanced surface roughness (Supporting Information S5) may result in a more hydrophilic membrane surface as well. [48] Therefore, the increased hydrophobicity for brominated membranes was a result of competing effects of bromine incorporation, carboxylic group formation, and roughness variation. NF270 became more hydrophobic after bromine exposure (Figure 2B, although chemical structure characterized by XPS and FTIR was not significantly altered), which was further verified by the increased permeabilities of hydrophobic hormones (Supporting Information S8). The increased contact angles for NF270 may be attributed to the

synergistic effects of trace bromine incorporation and the oxidation of amine groups to imine-like groups based on the oxidation mechanism of organic amine (reflected by the octanol-water partition coefficient of the terminal secondary amine and imine-like groups, -0.518 v.s. 0.402, calculated by Chemdraw)).[37, 49, 50]

NF90 became more negatively charged after it was exposed under bromine solutions (Figure 2C). Zeta potential for brominated NF90 under various pH conditions showed the similar trend (increased charge density) compared with that for a virgin one (Supporting Information S9). The negative charge for the fully-aromatic polyamide membranes is mainly attributed to the deprotonation of carboxylic groups. [4] A more negatively charged membrane surface may imply more carboxylic groups, which was experimentally verified by the calcium binding tests (surface Ca content increased from 0.5% for virgin membranes to 0.7% for brominated ones, see Supporting Information S6). Notably, the negative charge was nearly doubled at 10 mg/L bromine and further increase of bromine concentration to 500 mg/L only contributed to a minor further increase in surface charge, which indicate that membrane degradation mechanisms under mild and severe bromination conditions might be different. The minor increase of charge density for NF270 (Figure 2C) might be a result of the decreased content of –NH groups induced by bromine substitution and oxidation of the un-crosslinked –NH groups. [38, 51]

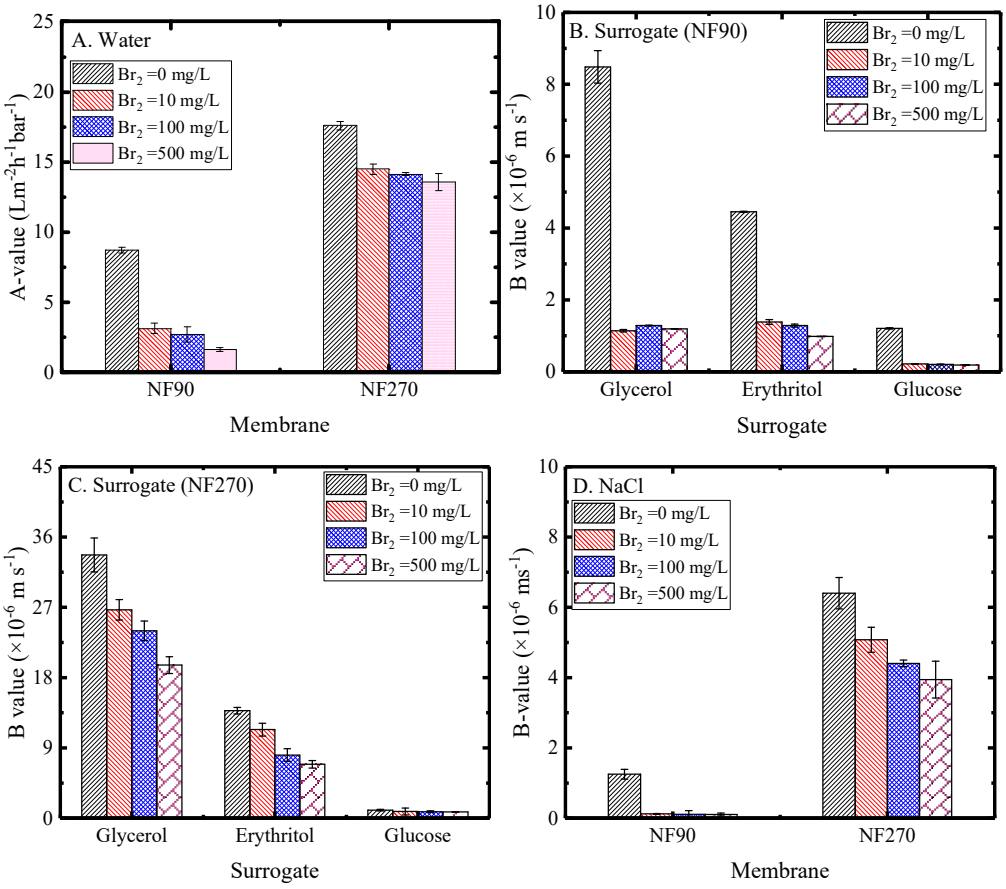

Figure 3. Effect of bromination on water permeability (A) and solute permeability (B, C, D) for NF90 and NF270. Membranes were exposed to bromine at 0, 10, 100, and 500 mg/L for 48 h, pH 7.5, 25 ºC. The feed water was DI water (A), 200 mg/L of each surrogate (B, C), and 5 mM NaCl (D), respectively. Other conditions for filtration experiments were: 100 psi, pH 7.5, 25 ºC. The error bars represented the range based on two independent experiments.

Effect of bromination on membrane filtration performance

Water permeability (A-value) and solute permeability (B-value) were used to evaluate the intrinsic membrane properties affected by bromination. The real rejection was used to calculate B-value to eliminate the effect of concentration polarization (Supporting Information S2). Figure 3A shows that pure water permeability of NF90 was reduced by 64% after it was exposed under 10 mg/L bromine for 48 h. Only another 18%

387 reduction was observed even if the bromine concentration was increased up to 500
388 mg/L. A similar but less significant decreasing trend was observed for NF270, which
389 should be a result of the weaker bromine attack ability to PIP-based polyamide
390 membranes. The degree of variation for water permeability under different bromine
391 conditions showed the similar trend for surrogate rejection tests (Supporting
392 Information S10). The less wettability (Figure 2B) and reduced effective pore radii (see
393 further discussion in the following paragraph, Figure 2D) of brominated membranes
394 should be responsible for the reduced water permeability.
395
396 Three neutral surrogate compounds with a molecular weight range of 92–180 mg/L
397 were used to probe the potential change of effective membrane pore radii induced by
398 bromination, since size exclusion is the dominant rejection mechanism for neutral
399 solutes. For virgin NF90 and NF270, the solute permeability was decreased with the
400 increased molecular sizes and the decreased effective membrane pore radius (Figure
401 3B, C), which verifies that the rejection of neutral solutes was primarily based on size
402 exclusion. The permeabilities of NF90 decreased by 87%, 69%, and 82% for glycerol,
403 erythritol, and glucose, respectively, under a mild bromination condition (10 mg/L).
404 Only a minor further decline of permeabilities (1%–9%) was observed under severe
405 bromination conditions (100 and 500 mg/L). A solute transport model commonly used
406 to access the effective membrane pore radius was applied to evaluate the impact of
407 bromination on membrane tightness.[41, 52] The effective pore radius of NF90 decreased

from 0.31 nm to 0.29 nm at 10 mg/L bromine and then remained constant after further exposure (Figure 2D). The competing effects of hydrolysis promoted pore opening and steric hindrance induced pore blocking might be responsible for the effective pore radius variation. The effective pore radius of NF270 decreased from 0.40 nm to 0.37 nm, which might be resulted from the synergistic effects of bromine incorporation induced steric hindrance and the structural compression caused by the cleavage of hydrogen bonds induced by the disappearance of –NH groups. [38]

The permeability of charged NaCl by NF90 was reduced by 90% after it was exposed to 10 mg/L bromine (Figure 3D). The enhanced electrostatic repulsion and reduced pore opening under a mild bromination condition made synergistic contributions to the reduced passage of NaCl, given that charged solutes are rejected mainly by size exclusion and charge interaction. A further slight decrease of 2% for NaCl passage under a severe bromination condition (500 mg/L) might be attributed only to the further slightly increased electrostatic repulsion (Figure 2C). For NF270, NaCl permeability was reduced by 21% and 38% under 10 and 500 mg/L, respectively.

In general, A- and B-values were decreased for brominated NF90 and NF270 (Figure 3), which indicates that both water and solutes became less permeable via membrane pore channels. Notably, the membrane performance was significantly affected under a mild bromination condition (10 mg/L) and only further slightly affected under severe

bromination conditions (100 and 500 mg/L). The A/B value was further evaluated to determine the effect of bromination on water-solute selectivity [53]. The significantly increased water-solute selectivity (A/B) (both surrogates and NaCl) for brominated NF90 demonstrated a greater reduction of solute permeability (B-value) compared with water permeability (A-value) (Supporting Information S11). [53-55] However, the partial A/B value for brominated NF270 shows different trends compared to that of brominated NF90, which could be attributed to the different bromination mechanism for these two membranes (see further discussions in section of possible degradation mechanism).

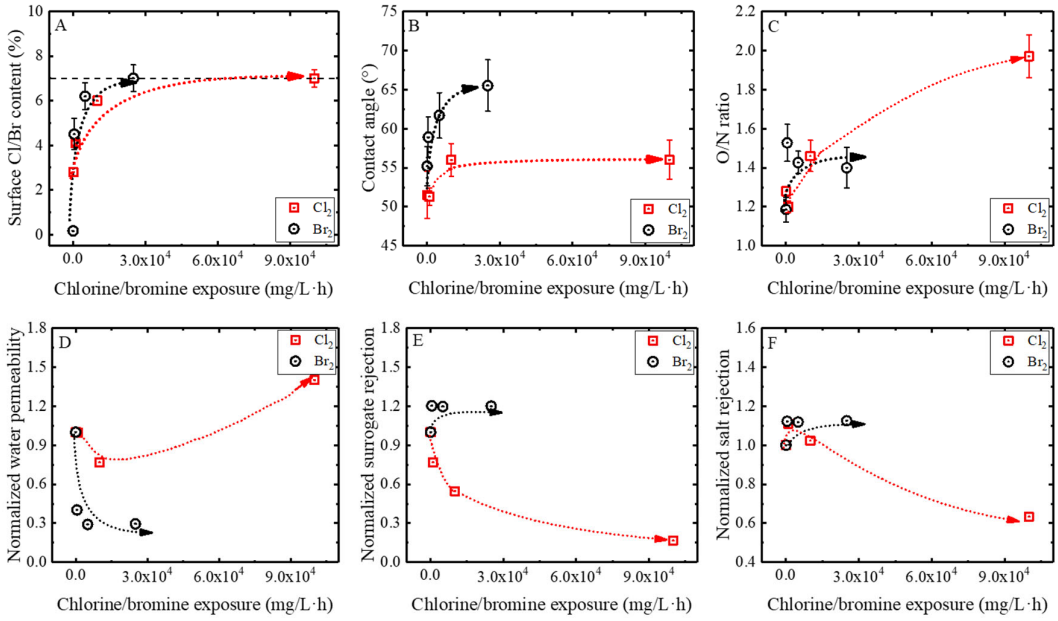

Figure 4. The surface chlorine or bromine content (A), contact angle (B), O/N ratio (C), normalized water permeability (D), surrogate rejection (E) and salt rejection (F) of NF90 exposed to various chlorine and bromine conditions. The normalization was obtained using a performance parameter of a chlorinated/brominated membrane divided by that of a virgin membrane. Data for membrane chlorination was obtained from a reference.[12]

Comparison between membrane chlorination and bromination

Bromine and chlorine are two most dominant oxidizing agents for biofouling control and water disinfection. Compared with the commonly used chlorine, bromine has been proven as a more efficient bactericide, especially under neutral and alkaline conditions.[56] The comparison between membrane chlorination and bromination will be beneficial for selecting oxidizing agents properly and taking effective actions to minimize membrane degradation. The data for NF90 chlorination was extracted from a reference.[12] The comparison for physicochemical properties and filtration performance was based on the CT concept, which is commonly used to access membrane tolerance.[12, 32] Our experiments also verified that membranes underwent similar extent of degradation under the same CT despite their different bromine concentrations, suggesting that the degradation phenomenon is kinetically controlled (Supporting Information S12). The bromine showed a relatively higher ability to incorporate with membrane materials than chlorine (Figure 4A), which partially contributes to a more hydrophobic surface (Figure 4B). Considering that the pK_a values of hypochlorous acid and hypobromous acid are 7.5 and 8.6, respectively, more HOBr than HOCl (94% vs. 50%, the stronger electrophilic oxidizing agents than OBr^- and OCl^-) was formed at pH = 7.5 under a given chlorine/bromine concentration (Supporting Information S13). Other researchers similarly found the lower halogenation rate of organic compounds and bulk membrane materials by chlorine than bromine.[13, 15] The more hydrophobic bromine than chlorine (reflected by octanol–water partition coefficients of 0.82 and 0.49 as logP for HOBr

467 and HOCl, respectively, data from ChemDraw) contributes to a more hydrophobic
468 halogenated NF90 as well.[13] The O/N ratio was increased from 1.2 to 2.0 under a severe
469 chlorination condition (1×10^5 mg/L·h, Figure 4C), which demonstrates a severe loss of
470 crosslinking caused by hydrolysis of polyamide due to the strong electron negativity of
471 chlorine. The O/N ratio appears to be less affected by bromination, despite that the more
472 bromine can be incorporated in the polyamide layer (Figure 4A).
473
474 It is worth noting that bromination and chlorination resulted in the opposite variation
475 trends for water permeability and neutral surrogate rejection (Figure 4D, E). The
476 increased water permeability and decreased surrogate rejection after chlorination have
477 been attributed mainly to the reduced cross-linking degree (a more open membrane
478 structure, Figure 4C) although the increased hydrophobicity played a competing role.
479 [12] By contrast, the weakened water permeability and strengthened surrogate rejection
480 for brominated membranes might be attributed to a synergistic result of reduced
481 hydrophilicity (55.2° vs. 65.5°) and reduced effective membrane pore radii (0.31 nm vs.
482 0.29 nm, under 500 mg/L bromine, Figure 2B, D). Compared with chlorinated
483 membranes, brominated membranes were less hydrolyzed (see the O/N ratios in Figure
484 4C). Meanwhile, bromine atoms are much bulkier than chlorine atoms, which would
485 promote a stronger steric hindrance effect and thus reduce the effective membrane pore
486 radius. The effective pore radius obtained by the filtration tests of neutral solutes is
487 therefore more suitable to evaluate the net effect on membrane opening. The opposite

trends for membrane opening caused by chlorination and bromination might be due to a smaller size and a less amount of chlorine compared with bromine but with greater extent of hydrolysis for the former. The different trends for NaCl rejection under mild and severe chlorination conditions were attributed to the competing effects of cross-linking degrees and charge density of polyamide membranes (Figure 4F).[12] For example, the effect of reduced cross-linking (reduce rejection) neutralized the effect of enhanced charge density (increase rejection), which eventually resulted in a ~37% reduction in NaCl rejection under a severe chlorination condition (1.0×10^5 mg/L·h). However, the increased charge density and membrane tightness induced by bromination would simultaneously contribute to enhanced NaCl rejection (Figure 2C, D and Supporting Information S14). In other words, the opposite variation trends for membrane opening caused by bromination and chlorination were primarily responsible for the different trends for NaCl rejection.

Table 2 The physicochemical properties (including the effective pore radius, zeta potential and hydrophilicity) of fully aromatic polyamide membranes affected by N-bromination and ring-bromination, and water, NaCl and surrogate permeability affected by these physicochemical properties.

	N-bromination				Ring-bromination			
	Effective pore radius	Zeta potential	Hydrophilicity	Overall	Effective pore radius	Zeta potential	Hydrophilicity	Overall
Membrane physicochemical properties	↓	↑	↓	/	—	—	↓	/
Water permeability	↓	—	↓	↓↓	—	—	↓	↓*
NaCl permeability	↓	↓	/	↓↓	—	—	—	—
Surrogate permeability	↓	—	↓	↓↓	—	—	↓	↓*

Notes: The symbols of "↑", "↓", and "—" referred to an increase, a decrease, and an unaffected trend, respectively. The blank marked with duplicated symbols indicated a remarkable change. The symbol of "*" referred to a minor variation.

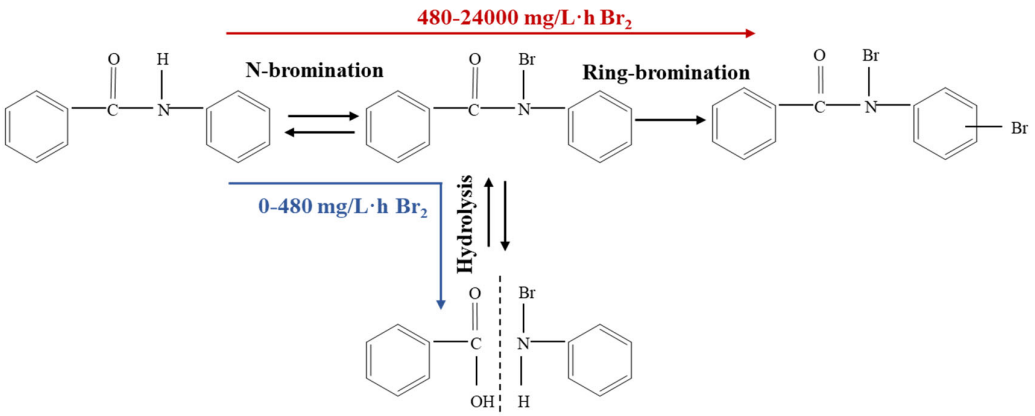

Figure 5. Possible degradation mechanism of fully aromatic polyamide membranes by bromine.

Possible degradation mechanism of polyamide membranes by bromine

N-chlorination and chlorination-promoted hydrolysis are the commonly proposed degradation mechanism of polyamide membranes (i.e., NF90) by chlorine.[12, 32, 57] Similarly, N-bromination, which is reflected by bromine incorporation (Figure 1A, C) and the shift and disappearance of three characteristic bands (Figure 2A), made membranes more hydrophobic under a mild bromination condition (10 mg/L) (Table 2). Bromination-promoted hydrolysis resulted in the formation of carboxyl groups (reflected by an increased O/N ratio and calcium content, Figure 1D and Supporting Information S6), which reduced the cross-linking degree (pore opening) and increased charge density (Figure 2C). Meanwhile, the higher steric hindrance of bromine than that of hydrogen may cause pore blocking after N-bromination. The reduced permeability for neutral solutes indicated that the steric hindrance of bromine dominates over the hydrolysis effect, which results in a reduction of the effective pore radius from

0.31 nm to 0.29 nm. In addition, the reduced hydrophilicity of membrane surfaces was partially responsible for the reduced permeability for those hydrophilic surrogates. The filtration tests for three hydrophobic hormones showed that their permeability was less affected than those hydrophilic surrogates after mild bromination. The permeability of hydrophobic hormones and hydrophilic surrogates was reduced by 63% and 83% on average, respectively, after mild bromination (Supporting Information S8, Figure 3B). It implies that a more hydrophobic pore channel may somehow hinder the transport of hydrophilic solutes. Therefore, the more hydrophobic and tighter membrane surface was responsible for the reduced water permeability. The enhanced NaCl rejection was a combined result of enhanced size exclusion and charge repulsion. Although N-halogenation and halogenation-promoted hydrolysis may occur regardless whether the fully aromatic polyamide membranes were exposed to chlorine or bromine, the different reaction intensity (the amount of incorporated halogen) and physicochemical properties for halogens (e.g., atomic size and hydrophilicity) may result in the opposite trends for membrane performance.

Under severe bromination conditions (100 and 500 mg/L), the further bromine incorporation resulted in a more hydrophobic membrane surface for NF90. However, the membrane tightness was less further altered (nearly similar O/N ratio and effective pore radii after mild and severe bromination, Figure 1D, 2D). The minor further reduction of water permeability can be attributed solely to the enhanced hydrophobicity.

It is also reasonable to observe the similar NaCl permeability under minor and severe bromination conditions (Figure 3D) since size exclusion and charge repulsion were similarly affected (Figure 2C, D). We speculate that ring-bromination in addition to N-bromination occurred under severe bromination conditions (Figure 5). The CT rather than exposure concentration and time determines the membrane degradation (Supporting Information S12) may indicate that membranes exposed under bromine even at a low concentration may undergo ring-bromination after a long exposure duration. Ring-bromination seemed to have a much lower reaction rate than N-bromination, given that the chemical changes started more probabilistically with N-bromination than ring-bromination (reflected by less than doubled bromine incorporation even with 50 times' higher exposure intensity, Figure 1C). In conclusion, ring-bromination led to further bromine incorporation and a more hydrophobic membrane surface, while did not significantly alter membrane charge density and tightness. Therefore, ring-bromiantion had a minor effect on membrane filtration performance. Ring-chlorination appears to be difficult to occur given that chlorine is less reactive than bromine.[15] The physicochemical properties (including the effective pore radius, zeta potential and hydrophilicity) affected by N-bromination and ring-bromination and their influences on water and solute permeability are presented in Table 2 to assist the overall mechanical understanding for the bromination of fully aromatic polyamide membranes.

Despite the generally similar but less significant deteriorated filtration performance of NF270 compared to NF90, the degradation pathway of PIP-based semi-aromatic polyamide membranes by bromine may require a different explanation. Although the current technologies (i.e., XPS, FTIR) seem insufficient to characterize the variation of surface chemistry for NF270, the reaction pathway was speculated based on chlorination mechanism proposed by Liu et al. [38] The absence of amide protons in semi-aromatic polymer chains of NF270 could account for its low bromine incorporation.[58, 59] Meanwhile, the un-crosslinked nitrogen atoms in secondary amines can be brominated and oxidized to form hydroxylamine,[38] and further dehydrated to form imine-like substances (Supporting Information S15).[58, 60, 61] The oxidation of amine groups would lead to the cleavage of secondary amine.[38] The trace amount of bromine on membrane surfaces and the oxidation of amine groups resulted in a more hydrophobic membrane surface (Figure 2B). Meanwhile, the steric hindrance induced by bromine incorporation and the structural compression caused by cleavage of hydrogen bonds induced by the disappearance of –NH groups may make the membrane tighter (reflected by the decreased effective pore radii in Figure 2D). The decreased hydrophilicity and smaller effective pore radius of membranes could account for the reduced permeability for water and neutral surrogates. The enhanced charge density and increased tightness of membranes could make synergistic effects on the decreased NaCl permeability. Nevertheless, the reaction between bromine and monomers (i.e., trimesoyl chloride and piperazine for NF270 [28]) and some advanced characterization

methods should be attempted in the future to confirm the above mechanism.

Implications

This study investigated the effect of bromine on physicochemical properties and filtration performance of polyamide membranes. Bromine incorporation to NF90 led to a more negatively charged and hydrophobic surface and a reduced effective pore radius under a mild bromination condition. This phenomenon resulted in a sharp decrease for permeabilities of water and solutes. N-bromination and bromination-promoted hydrolysis were the proposed degradation pathways, based on the shift and disappearance of three characteristic bands, and the increased O/N ratio and calcium content determined by XPS and FTIR. Compared with mild-brominated membranes, the hydrophobicity further increased and charge density and effective pore radii kept nearly unchanged for NF90 after severe bromination. Only a minor further reduction for water and neutral solute permeabilities was observed, which is supposed as a result of further ring-bromination. The membrane filtration performance induced by chlorine and bromine was significantly different. The different trends/degrees for halogen incorporation and its induced variation of membrane properties (e.g., membrane opening) might be due to a smaller size and a less amount of chlorine compared with bromine incorporated with bulk membrane materials (the effect of steric hindrance by halogen incorporation).

607 The exposure of polyamide membranes under various water conditions with different
608 halogenation ingredients (i.e., HOBr and HOCl) can affect membrane performance (i.e.,
609 membrane selectivity and permeability) in a different way. The precise correlation
610 between the changes in membrane physicochemical properties and filtration
611 performance and thereafter the proposal of the underlying degradation mechanisms will
612 assist the optimization of membrane-based treatment process and guide the next
613 generation of oxidant-resistant membrane materials. For example, free chlorine is not
614 recommended for seawater desalination process (with abundant bromine ions, the
615 formation of free bromine), given that the mild bromine exposure of polyamide
616 membranes will lead to severe flux decline. Although the studies were performed for
617 NF membranes, the bromination mechanisms of NF90 may be also relevant to RO
618 membranes since the latter adopts a similar fully aromatic polyamide chemistry. [28, 29]
619 Additional studies are also needed to further explore the bromination and chlorination
620 mechanisms for semi-aromatic polyamide membranes in view of relatively fewer
621 reports compared to fully aromatic counterparts.
622

623 ## Acknowledgements

624 This study was sponsored by the Natural Science Foundation of Shanghai
625 (19ZR1412800) and the National Key R&D Program (2019YFC0408202).
626

Appendix A. Supplementary data

Supplementary data related to this article can be found in the online version.

S1. Chemical structures for NF90 and NF270; S2. Water permeability (A-value) and solute permeability (B-value); S3. SEM images for the surfaces of virgin and brominated NF90 and NF270; S4. AFM images for virgin and brominated NF90 and NF270; S5. The average root-mean-square roughness (R_{rms}) for virgin and brominated NF90 and NF270; S6. Surface element content for virgin and brominated NF90 and NF270; S7. ATR-FTIR absorption spectra for virgin and brominated NF270; S8. Effect of bromination on hormone permeability for NF90 and NF270; S9. Effect of bromination on zeta potential for NF90 under various pH; S10. Effect of bromination on water permeability for NF90 and NF270; S11. Correlating A-value with B-value, and A/B value with bromination conditions for NF90 and NF270; S12. Effect of CT on water and solute permeability for NF90; S13. The species distribution of hypochlorous acid and hypobromous acid under different pH conditions; S14. Effect of bromination on NaCl rejection for NF90 and NF270; S15. Proposed degradation pathways of semi-aromatic polyamide membrane NF270 by bromine

References

(1) Ridgway, H. F.; Orbell, J.; Gray, S. Molecular simulations of polyamide membrane materials used in desalination and water reuse applications: Recent developments and future prospects. *J. Membr. Sci.* **2017,** *524*, 436-448.

(2) Zargar, M.; Jin, B.; Dai, S. An integrated statistic and systematic approach to study correlation of synthesis condition and desalination performance of thin film composite membranes. *Desalination.* **2016,** *394*, 138-147.

(3) Lee, K. P.; Arnot, T. C.; Mattia, D. A review of reverse osmosis membrane materials for desalination-development to date and future potential. *J. Membr. Sci.* **2011,** *370*, 1-22.

(4) Kwon, Y.-N.; Leckie, J. Hypochlorite degradation of crosslinked polyamide membranes: I. Changes in chemical/morphological properties. *J. Membr. Sci.* **2006,** *283*, 21-26.

(5) Ling, R.; Yu, L.; Pham, T. P. T.; Shao, J.; Chen, J. P.; Reinhard, M. The tolerance of a thin-film composite polyamide reverse osmosis membrane to hydrogen peroxide exposure. *J. Membr. Sci.* **2017,** *524*, 529-536.

(6) Gohil, J. M.; Suresh, A. K. Chlorine attack on reverse osmosis membranes: Mechanisms and mitigation strategies. *J. Membr. Sci.* **2017,** *541*, 108-126.

(7) Tucker, G. S.; Featherstone, S. *Essentials of thermal processing*. John Wiley & Sons: 2011.

(8) Nalepa, C. J. 25 Years Of Bromine Chemistry In Industrial Water Systems: A Review. NACE International 04087. In NACE International: 2004.

(9) Moffa, P. E.; Davis, D. P.; Somerlot, C.; Sharek, D.; Gresser, B.; Smith, T. Alternative disinfection technology demonstrates advantages for wet weather applications - a pilot study of powdered bromine technology. *Proc. Water Environ. Fed.* **2006,** *12*, 1202-1218.

(10) Anderson, A. C.; Reimers, R. S.; Dekernion, P. A brief review of the current status of alternatives of chlorine disinfection of water. *Am. J. Public Health.* **1982,** *72*, 1290-1293.

(11) Verbeke, R.; Gómez, V.; Vankelecom, I. F. J. Chlorine-resistance of reverse osmosis (RO) polyamide membranes. *Prog. Polym. Sci.* **2017,** *72*, 1-15.

(12) Van Thanh, D.; Tang, C. Y.; Reinhard, M.; Leckie, J. O. Effects of Chlorine Exposure Conditions on Physiochemical Properties and Performance of a Polyamide Membrane-Mechanisms and Implications. *Environ. Sci. Technol.* **2012,** *46*, 13184-13192.

(13) Suzuki, T.; Tanaka, R.; Tahara, M.; Isamu, Y.; Niinae, M.; Lin, L.; Wang, J.; Luh, J.; Coronell, O. Relationship between performance deterioration of a polyamide reverse osmosis membrane used in a seawater desalination plant and changes in its physicochemical properties. *Water Res.* **2016,** *100*, 326-336.

(14) Downs, A. J.; Adams, C. J. The Chemistry of chlorine, bromine, iodine and astatine: pergamon texts in inorganic chemistry, Vol.7. *Elsevier.* **2017**.

(15) Acero, J. L.; Piriou, P.; von Gunten, U. Kinetics and mechanisms of formation of bromophenols during drinking water chlorination: Assessment of taste and odor development. *Water Res.* **2005,** *39*, 2979-2993.
(16) Westerhoff, P.; Chao, P.; Mash, H. Reactivity of natural organic matter with aqueous chlorine and bromine. *Water Res.* **2004,** *38*, 1502-1513.
(17) Sandín, R. Relationship between hydraulic propertites and surface characterization of oxdized membranse in sea water. *Desalination Water Treat.* **2013,** *15*, 198-204.
(18) Kwon, Y. -N.; Joksimovic, R.; Kim, I. C.; Leckie, J. O. Effect of bromide on the chlorination of a polyamide membrane. *Desalination.* **2011,** *280*, 80-86.
(19) Davies, M. Myeloperoxidase-derived oxidation: mechanisms of biological damage and its prevention. *J. clin. biochem. nutr.* **2010,** *48*, 8-19.
(20) Sharma, V. K.; Rokita, S. E. Oxidation of amino acids, peptides, and proteins: kinetics and mechanism. *John Wiley & Sons*. **2012**, *9*.
(21) Glater, J.; Zachariah, M. R. A mechanistic study of halogen interaction with polyamide reverse-osmosis membranes. *In ACS Publications*. **1985**.
(22) Alam, A. 1,3-Dibromo-5,5-dimethylhydantoin. *Synlett.* **2005,** *15*, 2403-2404.
(23) Chassaing, C.; Haudrechy, A.; Langlois, Y. ChemInform abstract: 1,3-dibromo-5,5-dimethylhydantoin, a useful reagent for aromatic bromination. *Tetrahedron Lett.* **1997,** *38*, 4415-4416.
(24) Sivey, J. D.; Arey, J. S.; Tentscher, P. R.; Roberts, A. L. Reactivity of BrCl, Br_2, BrOCl, Br_2O, and HOBr toward dimethenamid in solutions of bromide+ aqueous free chlorine. *Environ. Sci. Technol.* **2013,** *47*, 1330-1338.
(25) Sivey, J. D.; Bickley, M. A.; Victor, D. A. Contributions of BrCl, Br_2, BrOCl, Br_2O, and HOBr to regiospecific bromination rates of anisole and bromoanisoles in aqueous solution. *Environ. Sci. Technol.* **2015,** *49*, 4937-4945.
(26) Broadwater, M. A.; Swanson, T. L.; Sivey, J. D. Emerging investigators series: comparing the inherent reactivity of often-overlooked aqueous chlorinating and brominating agents toward salicylic acid. *Environ. Sci. Water Res. Technol.* **2018,** *4*, 369-384.
(27) Racar, M.; Dolar, D.; Spehar, A.; Kosutic, K. Application of UF/NF/RO membranes for treatment and reuse of rendering plant wastewater. *Process Saf. Environ. Prot.* **2017,** *105*, 386-392.
(28) Tang, C. Y. Y.; Kwon, Y. -N.; Leckie, J. O. Effect of membrane chemistry and coating layer on physiochemical properties of thin film composite polyamide RO and NF membranes I. FTIR and XPS characterization of polyamide and coating layer chemistry. *Desalination.* **2009,** *242*, 149-167.
(29) Tang, C. Y.; Kwon, Y.-N.; Leckie, J. O. Effect of membrane chemistry and coating layer on physiochemical properties of thin film composite polyamide RO and NF membranes II. Membrane physiochemical properties and their dependence on polyamide and coating layers. *Desalination.* **2009,** *242*, 168-182.
(30) Nghiem, L. D.; Schafer, A. I.; Elimelech, M. Removal of natural hormones by nanofiltration membranes: Measurement, modeling, and mechanisms. *Environ. Sci.*

Technol. **2004,** *38*, 1888-1896.
(31) Ettori, A.; Gaudichet-Maurin, E.; Schrotter, J.-C.; Aimar, P.; Causserand, C. Permeability and chemical analysis of aromatic polyamide based membranes exposed to sodium hypochlorite. *J. Membr. Sci.* **2011,** *375*, 220-230.
(32) Do, V. T.; Tang, C. Y. Y.; Reinhard, M.; Leckie, J. O. Degradation of polyamide nanofiltration and reverse osmosis membranes by hypochlorite. *Environ. Sci. Technol.* **2012,** *46*, 852-859.
(33) Moses, K. J.; Cohen, Y. Wettability of terminally anchored polymer brush layers on a polyamide surface. *J. Colloid interface Sci.* **2014,** *436*, 286-295.
(34) Abramson, H. Electrokinetic Phenomena and Their Application to Biology and Medicine. *The Chemical Catalog Company.* **1934**.
(35) Li, Y.; Yang, L.; Zhen, H.; Chen, X.; Cao, G. Determination of estrogens and estrogen mimics by solid-phase extraction with liquid chromatography-tandem mass spectrometry. *J. Chromatogr. B.* **2021,** *1168*, 122559.
(36) Surawanvijit, S.; Rahardianto, A.; Cohen, Y. An Integrated approach for characterization of polyamide reverse osmosis membrane degradation due to exposure to free chlorine. *J. Membr. Sci.* **2016,** *510*, 164-173.
(37) Xue, S. M.; Xu, Z. L.; Tang, Y. J.; Ji, C. H. Polypiperazine-amide nanofiltration membrane modified by different functionalized multiwalled carbon nanotubes (MWCNTs). *Acs Appl. Mater. Interfaces.* **2016,** *8*, 19135-19144.
(38) Liu, S.; Wu, C.; Hou, X.; She, J.; Liu, S.; Lu, X.; Zhang, H.; Gray, S. Understanding the chlorination mechanism and the chlorine-induced separation performance evolution of polypiperazine-amide nanofiltration membrane. *J. Membr. Sci.* **2019,** *573*, 36-45.
(39) Simon, A.; Nghiem, L. D.; Le-Clech, P.; Khan, S. J.; Drewes, J. E. Effects of membrane degradation on the removal of pharmaceutically active compounds (PhACs) by NF/RO filtration processes. J. *Membr. Sci.* **2009,** *340*, 16-25.
(40) Glater, J.; Hong, S. K.; Elimelech, M. The search for a chlorine-resistant reverse osmosis membrane. *Desalination.* **1994,** *95*, 325-345.
(41) Yang, L.; She, Q.; Wan, M. P.; Wang, R.; Chang, V. W.-C.; Tang, C. Y. Y. Removal of haloacetic acids from swimming pool water by reverse osmosis and nanofiltration. *Water Res.* **2017,** *116*, 116-125.
(42) Skrovanek, D. J.; Howe, S. E.; Painter, P. C.; Coleman, M. M. Hydrogen bonding in polymers: infrared temperature studies of an amorphous polyamide. *Macromolecules.* **1985,** *18*, 1676-1683.
(43) Socrates, G. Infrared and Raman characteristic group frequencies: tables and charts. *John Wiley & Sons*: 2004.
(44) Kwon, Y.-N.; Leckie, J. O. Hypochlorite degradation of crosslinked polyamide membranes: II. Changes in hydrogen bonding behavior and performance. *J. Membr. Sci.* **2006,** *282*, 456-464.
(45) Wu, S.; Zheng, G.; Lian, H.; Xing, J.; Shen, L. Chlorination and oxidation of aromatic polyamides. I. Synthesis and characterization of some aromatic polyamides. *J. Appl. Polym. Sci.* **1996,** *61*, 415-420.

(46) Avilés-Barreto, S. L.; Suleiman, D. Effect of single-walled carbon nanotubes on the transport properties of sulfonated poly (styrene–isobutylene–styrene) membranes. *J. Membr. Sci.* **2015,** *474*, 92-102.
(47) Idil Mouhoumed, E.; Szymczyk, A.; Schafer, A.; Paugam, L.; La, Y. H. Physico-chemical characterization of polyamide NF/RO membranes: Insight from streaming current measurements. *J. Membr. Sci.* **2014,** *461*, 130-138.
(48) Tao, M.; Xue, L.; Liu, F.; Jiang, L. An intelligent superwetting PVDF Membrane showing switchable transport performance for oil/water separation. *Adv. Mater.* **2014,** *26*, 2943-2948.
(49) Kang, G. D.; Gao, C. J.; Chen, W. D.; Jie, X. M.; Cao, Y. M.; Yuan, Q. Study on hypochlorite degradation of aromatic polyamide reverse osmosis membrane. *J. Membr. Sci.* **2007,** *300*, 165-171.
(50) Zhang, H. Z.; Xu, Z. L.; Tang, Y. J.; Ding, H. Highly chlorine-tolerant performance of three-channel capillary nanofiltration membrane with inner skin layer. *J. Membr. Sci.* **2017,** *527*, 111-120.
(51) Xu, J.; Wang, Z.; Wei, X.; Yang, S.; Wang, J.; Wang, S. The chlorination process of crosslinked aromatic polyamide reverse osmosis membrane: New insights from the study of self-made membrane. *Desalination.* **2013,** *313*, 145-155.
(52) Yang, L.; Zhou, J.; She, Q.; Wan, M. P.; Wang, R.; Chang, V. W. C.; Tang, C. Y. Role of calcium ions on the removal of haloacetic acids from swimming pool water by nanofiltration: Mechanisms and implications. *Water Res.* **2017,** *110*, 332-341.
(53) Yang, Z.; Guo, H.; Tang, C. Y. Y. The upper bound of thin-film composite (TFC) polyamide membranes for desalination. *J. Membr. Sci.* **2019,** *590*.
(54) Geise, G. M.; Park, H. B.; Sagle, A. C.; Freeman, B. D.; McGrath, J. E. Water permeability and water/salt selectivity tradeoff in polymers for desalination. *J. Membr. Sci.* **2011,** *369*, 130-138.
(55) Labban, O.; Liu, C.; Chong, T. H.; Lienhard, J. H. Relating transport modeling to nanofiltration membrane fabrication: Navigating the permeability-selectivity trade-off in desalination pretreatment. *J. Membr. Sci.* **2018,** *554*, 26-38.
(56) Yang, L.; Schmalz, C.; Zhou, J.; Zwiener, C.; Chang, V. W. C.; Ge, L.; Wan, M. P. An insight of disinfection by-product (DBP) formation by alternative disinfectants for swimming pool disinfection under tropical conditions. *Water Res.* **2016,** *101*, 535-546.
(57) Do.V. T.; Tang, C. Y. Y.; Reinhard, M.; Leckie, J. O. Effects of hypochlorous acid exposure on the rejection of salt, polyethylene glycols, boron and arsenic(V) by nanofiltration and reverse osmosis membranes. *Water Res.* **2012,** *46*, 5217-5223.
(58) Glater, J.; Hong, S.-k.; Elimelech, M. The search for a chlorine-resistant reverse osmosis membrane. *Desalination.* **1994,** *95*, 325-345.
(59) Kawaguchi, T.; Tamura, H. Chlorine-resistant membrane for reverse osmosis. I. Correlation between chemical structures and chlorine resistance of polyamides. *J. Appl. Polym. Sci.* **1984,** *29*, 3359-3367.
(60) Kang, G. D.; Gao, C. J.; Chen, W. D.; Jie, X. M.; Cao, Y. M.; Yuan, Q. Study on hypochlorite degradation of aromatic polyamide reverse osmosis membrane. *J. Membr.*

Sci. **2007,** *300*, 165-171.
(61) Zhang, H. Z.; Xu, Z. L.; Tang, Y. J.; Ding, H. Highly chlorine-tolerant performance of three-channel capillary nanofiltration membrane with inner skin layer. *J. Membr. Sci.* *527*, 111-120.